EARTHQUAKE RESPONSE OF REINFORCED CONCRETE STRUCTURES CONSIDERING THE DISCONTINUOUS FAILURE PROCESS TO COLLAPSE

by

Sukenobu Tani*, Setsuro Nomura**, Tomoya Nagasaka***,
Akira Hiramatsu****, and Isao Mochizuki****.

SYNOPSIS

Earthquake response of reinforced concrete structures is presented. This paper deals with the effects of various features of restoring force characteristics, which includes the whole hysteretic region to the extent of the state of ultimate collapse, of reinforced concrete structures.

First, the restoring force characteristics of braced frames and walled frames are obtained by experiments on the model specimens, the force being applied laterally and cyclically from the small displacement region to the state of ultimate collapse. Then, the method of idealizing the restoring force characteristics of reinforced concrete structures is described. The effects of the various properties of the restoring force characteristics that influence the one mass system's response to earthquakes are also mentioned.

INTRODUCTION

When the structures are subjected to both vertical load and horizontal load such as an earthquake motion, the structures would be suffering at each structural element due to the increasing displacement, and at last they would come to lose the resistance against the lateral load. In some of the worse cases, the structures would become unable to support even the vertical load and lose mechanical stability to entire collapse. These entire collapse cases could be seen in recent disastrous earthquakes, such as Hakodate Univ. at Tokachioki Earthquake 1968 Japan and Olieve View Hospital at San Fernando Earthquake 1971 U.S.A.

The vibrational behaviour of structures, that is induced by earthquake motion strong enough to fall into the state of collapse, might be a very complicated one. In this case, the behaviour should be affected with the dynamic properties i.e. the restoring force characteristics of whole region from small displecement to ultimate state of entire collapse.

Thus, to estimate precisely the aseismic safety of the structure, we must realize the restoring force characteristics throughout the whole region from beginning to end.

---

* Professor, Dept. of Architecture, Waseda Univ. Tokyo
** Associate Professor, Dept. of Architecture, Science Univ. of Tokyo
*** Lecturer, Dept. of Architecture, Tokai Univ. Tokyo
**** Graduate Student, Waseda Univ. Tokyo

Generally it is admitted that, when the structures are affected by the strong vibrational force, the structural failure proceeds, and as nearing the ultimate state, the effects due to both the increase of displacement and the alternation of cyclic external force are increasing. Under these circumstances, strength and stiffness of the structures are gradually reduced. Especially if the failure of reinforced concrete structures occurs in a brittle manner, the reduction of strength and stiffness would be more notable and load-displacement curve would become discontinuous. In such cases, the vibrational responses of the structures are thought to be no longer than simple behaviours.

On the other hand, up to this time, most of the earthquake responses have been calculated by adopting rather simplified models, such as Bi-linear model, Tri-linear model or Degrading stiffness model (1) (2) (3). However, it is desirable to show the adequate idealized model which describes the restoring force characteristics of reinforced concrete structures more precisely.

The authors have been studying the restoring force characteristics of reinforced concrete aseismic elements. As the result of this study, we have noted that the restoring force characteristics of reinforced concrete structures could be represented by composing a skeleton curve and Normalized Characteristic Loop (NCL model) (2) for the region up to about 70% of maximum strength. This paper deals with the test results experimented recently by the authors on the restoring force characteristics in the ultimate region of reinforced concrete model specimens. we will show that the restoring force characteristics can be represented by NCL model with consideration of cyclic deterioration effects even in the ultimate region.

EXPERIMENTAL RESULTS

The outlines of loading apparatus and test specimens, braced frames and walled frames are shown Fig. 1 and Fig. 2, respectively. Material properties are listed in table 1. Horizontal displacement D relative to its base was measured by 1/100 dialgage and horizontal load P by load cell, respectively. Vertical load N was imposed on the tops of both columns, totally 6 ton which corresponds with normal stress 47 kg/cm^2. Ten braced frame specimens were used in six test programs (B-1~B-VI) while six walled frame specimens were in three test programs (W-I~W-III). Open frames were also experimented (F-I~F-III). Some of the typical P-D curves are shown in Fig. 3-1~Fig. 3-9. Fig. 4-1 and Fig. 4-2 show the ultimate state of each type of frames. In this paper we will pay attention to only P-D curves from the point of view to idealize the restoring force characteristics model.

According to the tests of braced frames, when reaching its maximum strength point, failure of each specimen occured brittlely at compressive bracing, and at the same time, the restoring force dropped abruptly. Thereafter, the restoring force increased as the displacement increased. The restoring force at this stage is approximately equal to the sum of the strength of reinforcements in tensile bracing plus that of the frame system which consists of columns and a beam. Displacement at the ultimate

state and the process to the ultimate state of all specimens were not the same, but every specimen can be considered to be a composed system of frame and tensile bracing.

Summary of braced frame experiment is as follows:

(1) Displacement at maximum strength is about 6 mm (10×10^{-3} rad) for all specimens.

(2) Reaching the point of maximum strength, the compressive bracing fractured brittlely and the restoring force dropped abruptly to the value which coincides approximately with the sum of each strength of frame and reinforcements in tensile bracing.

(3) In large displacement region (larger than about 6×10^{-3} rad), cyclic deterioration effects become notable.

(4) Even in the large displacement region ($100 \times 10^{-3} \sim 130 \times 10^{-3}$ rad) after the maximum strength point, the frame can still support vertical load.

(5) 5~10 cycles are required to cause failure in compressive bracing under the fixed load amplitude of about 90% of maximum strength.

(6) Due to the cyclic behaviour on one side of the region after reaching the maximum strength point, the strength of the other side decreases gradually.

The restoring force characteristics of walled frames are compared with those of braced frames. Displacements at maximum strength are different, which suggests to us the instability of the dynamic properties of walled frames. These facts are thought to be attributed to various processes of failure in walled frames contrally to rather simple failure mechanism of braced frames, in which the maximum strength is pertinent to compressive bracing failure only. So, when the restoring force drops at its maximum strength point, there is an abrupt jump-like phenominon in the case of braced frames. However, walled frames show more gradual reduction of strength, appearing as a continuous curve in the P-D relationship.

The cracks due to the shearing force progress into the column straightforwardly and this would weaken the column strength. These behaviours are undesirable for aseismic safety of the structures.

IDEALIZED MODEL FOR RESTORING FORCE CHARACTERISTICS

We have already reported about the restoring force characteristics model for the region before reaching the maximum strength (4) (5).

$$Q(D)=A\times(e^{-\eta D}-e^{-\xi D}) \quad .....(1)$$

Eq. 1 represents the skeleton curve after the maximum strength (2nd SC) which is comparable to those of the braced frames experimental results in Fig. 5. Fig. 6-1 shows the hysteresis loops of braced frames (B-III) normalized by each corresponding peak point. Fig. 6-2 shows the averaged normalized loop of those in Fig. 6-1. The model loop simulated to this averaged one is idealized by 10th order power expression as seen in Fig. 6-3. This idealized loop will be used in response calculations in the next section as the normalized characteristic loop in ultimate region (2nd NCL).

As illustrated in Fig. 7-1, the cyclic effect of external forces would cause the displacement amplitude to increase under the fixed load amplitude. We define K_i to be a temporal stiffness which reffers to the i th peak point, and the coefficient of stiffness reduction γ_i to be K_i/K_1. The relationship between log i and $\log\gamma_i^{-1}$ is generally said to be a linear one. This relationship of two braced frames (B-VI) is plotted in Fig. 7-2. Admitting the linear relationship between log i and $\log\gamma_i^{-1}$, we obtain Eq. 2 in which a is a proportional constant.

$$\log i = a\times\log\gamma_i^{-1} \quad .....(3)$$

In Fig. 7-2, the averaged value of a's is observed as about 0.1. Furthermore, if the strength in the ultimate region is to be constant Q_u Eq. 4 is held.

$$K_i = Q_u / D_i \quad .....(4)$$

Where D_i is the displacement of i th peak point. From Eq. 3 and Eq. 4, we obtain Eq. 5.

$$D_i = D_1 \times i^a \quad .....(5)$$

Hysteresis curve obtained by combining the 2nd skeleton curve of Eq. 1 and the normalized characteristic loop in Fig. 6-3 is illustraited in Fig. 8-1 where the cyclic deterioration effects are taken into account as expressed by Eq. 5. We can compare this idealized hysteresis behaviour with that of the experimental result shown in Fig. 8-2 (B-III).

EARTHQUAKE RESPONSE BEHAVIOUR

In this section, we will discuss the earthquake response behaviour affected by the two notable characteristics of the restoring force characteristics mentioned in the previous section. One is the effect of the discontinuous curve in the P-D relationship pertaining to brittle failure. 2nd is the cyclic deterioration effects in the large displacement region.

Equation of motion of a one mass system is expressed as Eq. 6.

$$m\cdot\ddot{X}+Q(X)=-m\cdot\ddot{Z} \qquad .....(6)$$

where m is the mass of the system, $\ddot{Z}$ is the ground acceleration and X is the displacement of the mass relative to its base, respectively.

NCL model is addopted as the restoring force function Q(X), and El-Centro 1940 NS (maximum 330 gal) accelerogram is used as an input data. Responses are calculated numerically by the 4th ordered Rung-Kutta method.

The curves shown in Fig. 9-1 are used as the 1st skeleton curve in the region before the maximum strength point and the 2nd skeleton curves. The initial stiffness of 1st skeleton curve is adjusted to have 0.6 sec. natural period. We define some parameters as follows, α is the ratio of the maximum strength Q_{u1} of the system to the weight m.g (g is the gravity acceleration) i.e. $Q_{u1}=\alpha\cdot m.g$, β is the ratio of maximum strength of 2nd skeleton curve Q_{u2} to Q_{u1} i.e. $Q_{u2}=\beta\cdot Q_{u1}$ and X_f is the displacement at which the brittle failure is to occur.

Fig. 9-2 shows the normalized characteristic loop used in the region before reaching the maximum strength point (1st NCL).

The displacement response wave under the assumption $X_f=\infty$ and the associated restoring force characteristics are shown in Fig. 10-1 and Fig. 10-2, respectively. And its maximum displacement is $X_{max}=10.2$ c.m. at 4.8 sec. from the beginning of earthquake motion. Fig. 11 shows the relationship between the maximum displacement and the coefficient C, defined as $X_f=C\cdot X_{max}$. And also, Fig. 12-1 and Fig. 12-2 show the response waves and restoring force characteristics for the cases of $\beta=0.2$ and $\beta=0.4$ under the fixed value of $C=0.9$. Fig. 11 suggests to us that the maximum displacements are not so influenced by the coefficient C as by the parameter β. Especially, it is seen that when the β takes the large value, the maximum displacement is rather smaller than that of the case of $X_f=\infty$ shown in Fig. 10-1. This results are thought to be attributed to the fact that the larger hysteretic damping effect is expected from the 2nd normalized characteristic loop than that of the first normalized characteristic loop.

Furthermore, we could see that response displacement inclines remarkably, hence, the structure is to keep responding in the unsymmetric state. We also observe that when the brittle failure occurs at one side of the P-D curve, it can hardly reach the maximum strength point at the other side.

From these observation, we could say that the response displacement might become large, if β takes the small value, so the structural safety should be decreased.

Influence of the cyclic deterioration effects is observed by using the restoring force characteristics model, which is now composed by the 1st skeleton curve of Fig. 9-1 and the 1st normalized characteristic loop in Fig. 9-2. Eq. 5 is assumed to express the stiffness reduction

model in cyclic behaviours. The relationships between the maximum displacement and the parameter a are shown in Fig. 13. Note that the experimental value of a is thought to be between 0.1 and 0.3 approximately. From Fig. 13, we could say that the cyclic deterioration effects of actual structures would hardly make an influence on the response behaviours of reinforced concrete structures. One of the response behaviours α=0.4, a=0.1) is shown in Fig. 14. When comparing Fig. 14 with the response wave obtained by ignoring the deterioration effects in Fig. 10, little distinction between them is observed.

From the response calculations of various restoring force characteristics, we could summarize as follows:

(1) When the structure falls into brittle failure and the restoring force drops abruptly under the vibrational force, the response characteristics are no more than simple and symmetric.

(2) Once the brittle failure occurs in one direction, the failure has a tendency to keep on proceeding in the same direction and failure on the opposite direction might hardly occur.

(3) When the amount of strength reduction is large (β is small), the displacement response should be expected to increase considerably.

REFERENCES

(1) R. W. Clough "Effects of Stiffness Degradation on Earthquake Ductility requirements". Report No. 66-14 S.M.R Univ. of Calif. 1966

(2) Y. Abe, J. Ogawa and A. Shibata "Earthquake Response of Reinforced concrete frame". Proc. Third JEES-1970 V-6

(3) T. Takeda, A. Sozen and N. N. Nielsen "Reinforced Concrete Response to Simulated Earthquakes" Proc. of the Third JEES-1970

(4) S. Tani, S. Nomura, T. Nagasaka and A. Hiramatsu "Study on Restoring Force Characteristics of Reinforced Concrete Structures (Static Analysis)" Third JEES-1970 V-7

(5) S. Tani, S. Nomura, T. Nagasaka and A. Hiramatsu "Study on Restoring Force Characteristics of Reinforced Concrete Structures (Non-linear Seismic Responses)" Third JEES-1970 V-8

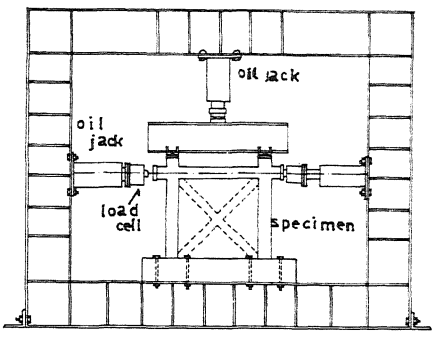

FIG.1 LOADING APPARATUS

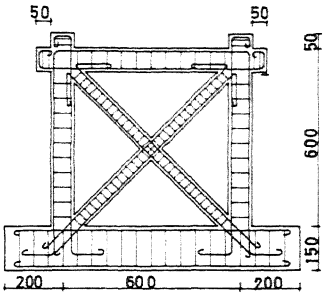

BRACED FRAME

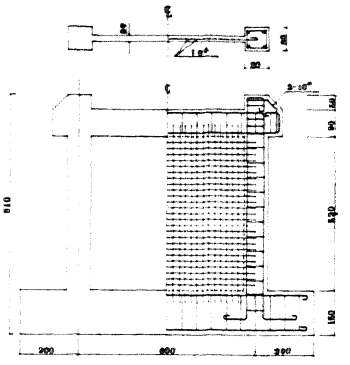

WALLED FRAME

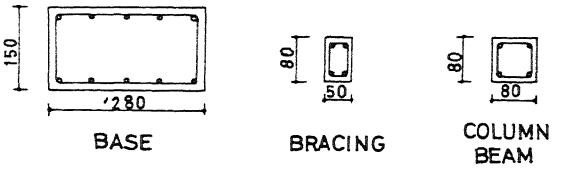

BASE BRACING COLUMN BEAM

FIG 2 TEST SPECIMENS

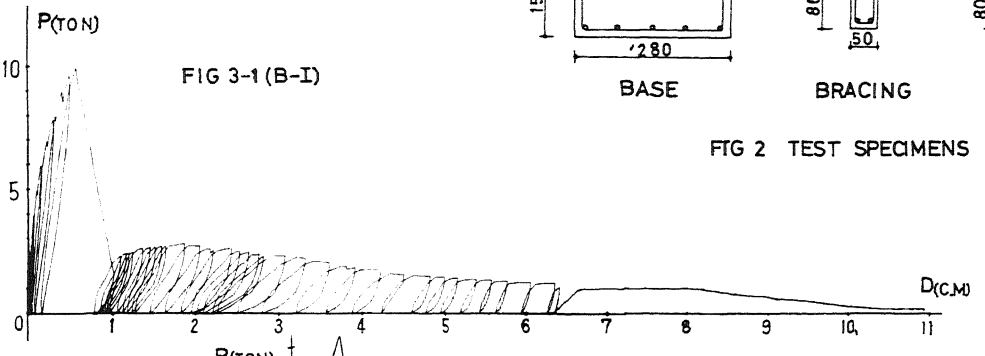

FIG 3-1 (B-I)

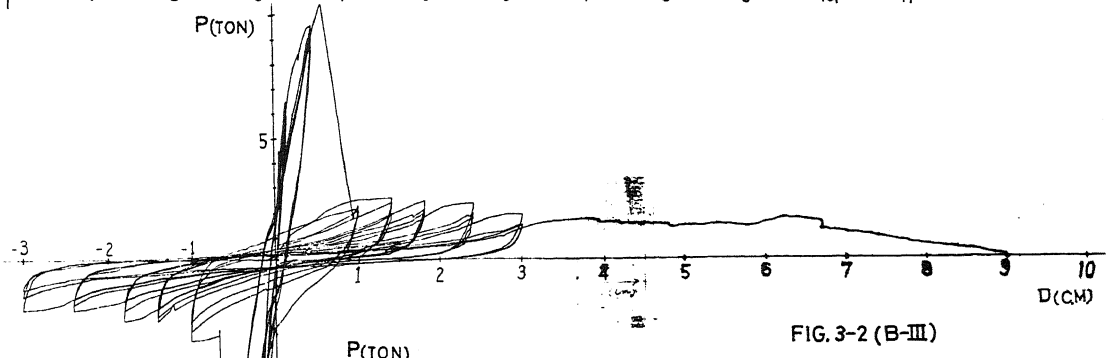

FIG. 3-2 (B-III)

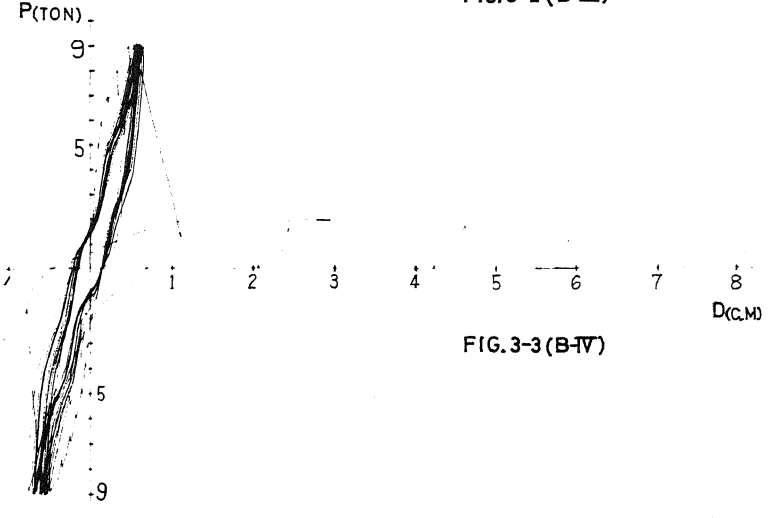

FIG. 3-3 (B-IV)

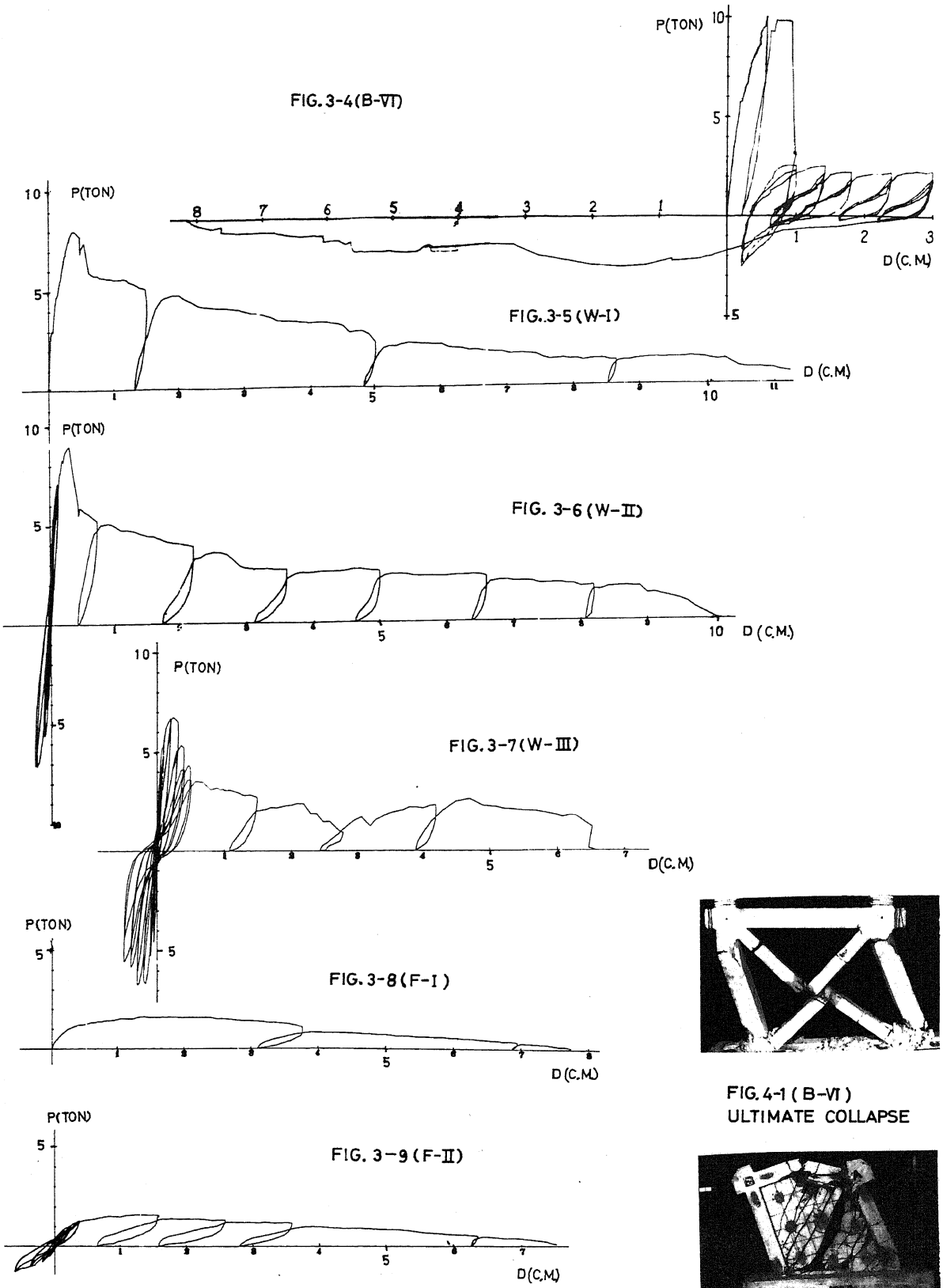

FIG. 3-4(B-VI)

FIG. 3-5 (W-I)

FIG. 3-6 (W-II)

FIG. 3-7 (W-III)

FIG. 3-8 (F-I)

FIG. 3-9 (F-II)

FIG. 4-1 (B-VI)
ULTIMATE COLLAPSE

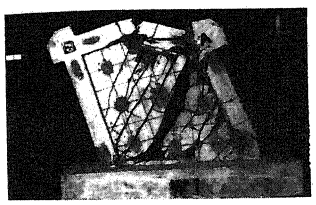

FIG.4-2 (W-I)
ULTIMATE COLLAPSE

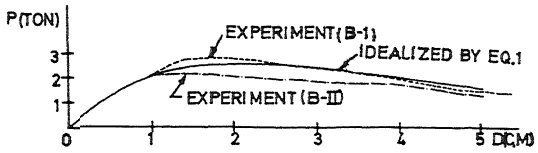

FIG. 5 COMPARISON OF 2ND SKELETON CURVE

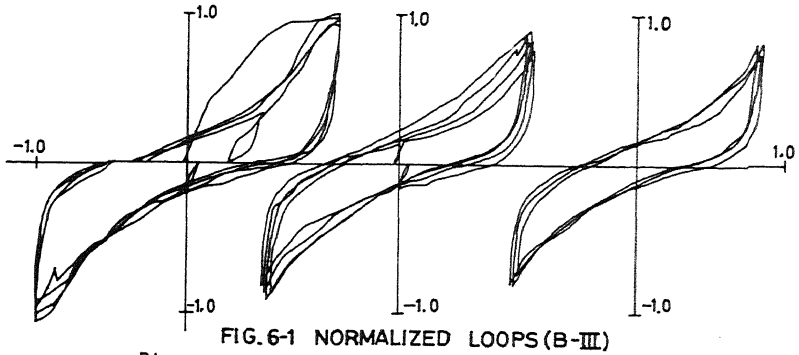

FIG. 6-1 NORMALIZED LOOPS (B-III)

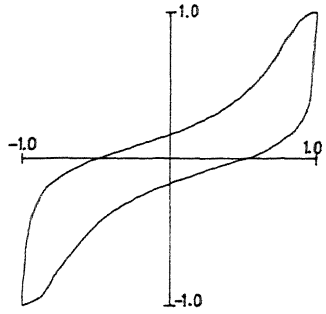

FIG. 6-2 AVERAGE LOOP

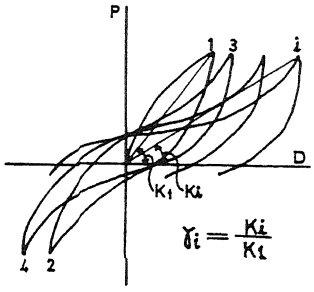

FIG. 7-1 STIFFNESS REDUCTION BY DETERIORATION EFFECT

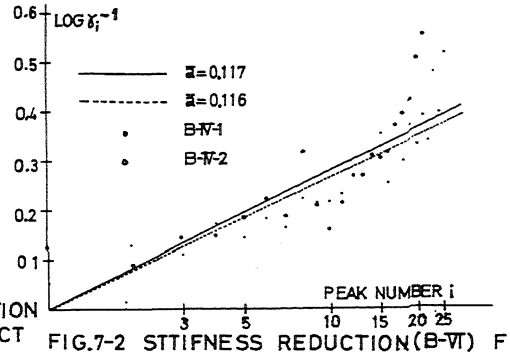

FIG. 7-2 STTIFNESS REDUCTION (B-VI)

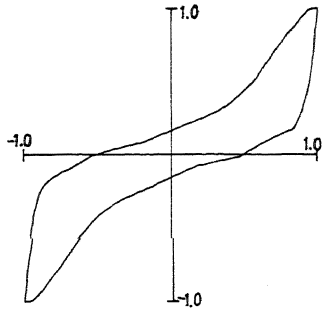

FIG. 6-3 IDEALIZED NORMALIZED CHARACTERISTIC LOOP

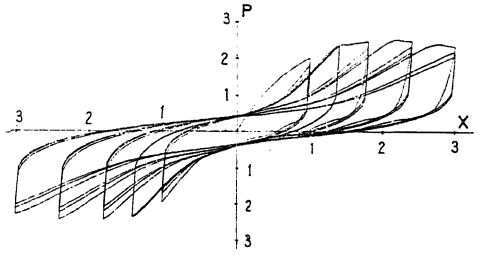

FIG. 8-1 IDEALIZED MODEL CONSIDERING CYCLIC DETERIORATION EFFECT

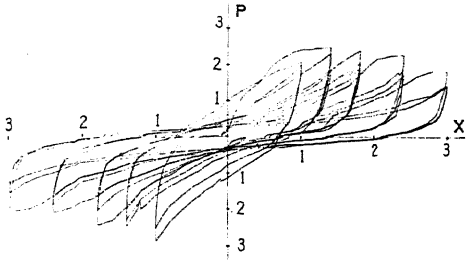

FIG. 8-2 EXPERIMENTAL RESULT (B-III)

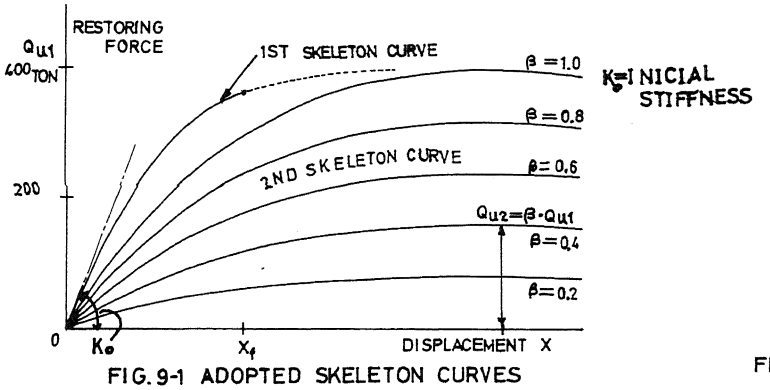

FIG. 9-1 ADOPTED SKELETON CURVES

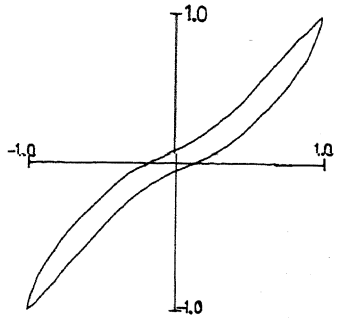

FIG. 9-2 ADOPTED 1ST NORMALIZED CHARACTERISTIC LOOP

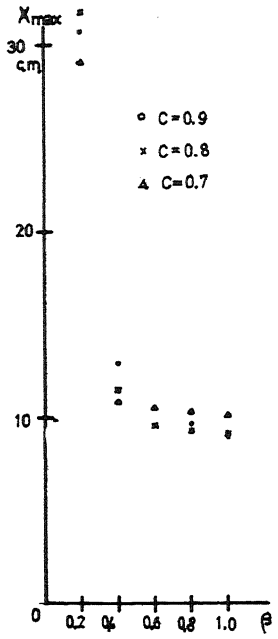

FIG.11 MAXIMUM DISPLACEMENT

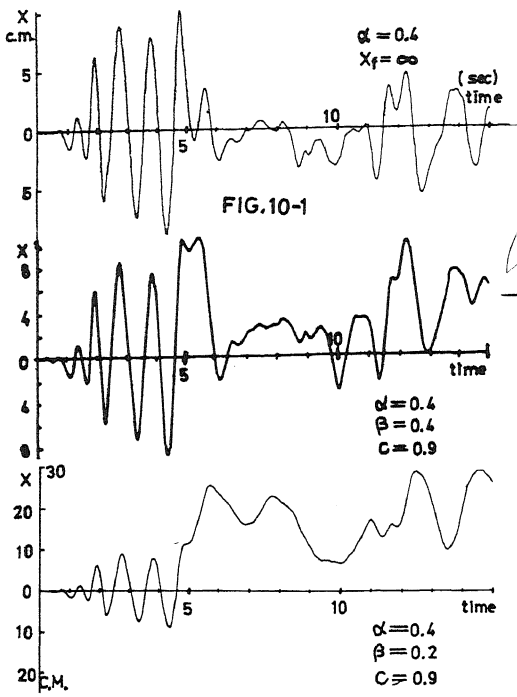

FIG.12-1 RESPONSE WAVES

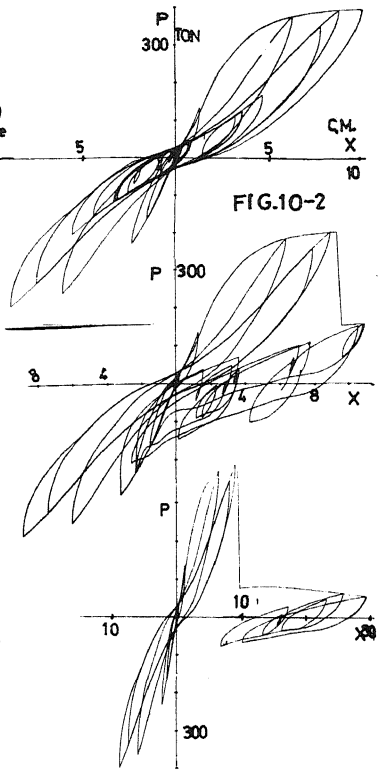

FIG.12-2 HYSTERESIS RESPONSES

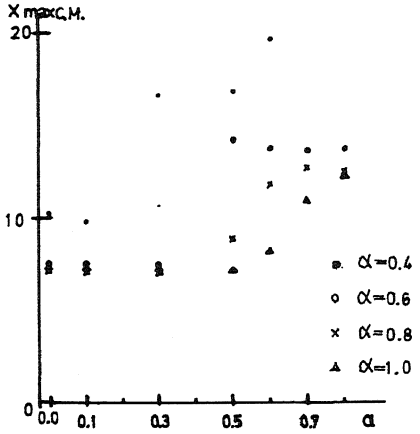

FIG.13 MAXIMUM DISPLACEMENT

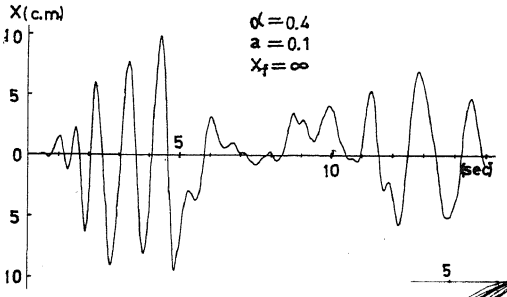

FIG.14-1 RESPONSE WAVES

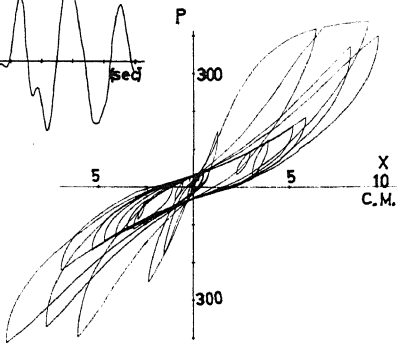

FIG 14 2 HYSTERESIS RESPONSE

TABLE 1 MATERIAL PROPERTIES

MORTATL			REINFORCEMENT			
young's modlus kg/cm²	compres. strength kg/cm²	tensile strength kg/cm²	type	young's modulus kg/cm²	compres strength kg/cm²	tensile strength kg/cm²
201	240	340	6φ	2.45×10^6	4750	5700
			8#	2.00×10^6	1800	——
			16#	2.20×10^6	——	3600